PAPER

An easy method of preparing ozone gas sensors based on ZnO nanorods†

Ariadne C. Catto,[a] Luís F. da Silva,*[b] Caue Ribeiro,[c] Sandrine Bernardini,[d] Khalifa Aguir,[d] Elson Longo[b] and Valmor. R. Mastelaro[a]

One-dimensional (1D) ZnO nanorod-like structures were successfully grown *via* a hydrothermal method to be used as an ozone gas sensor. X-ray diffraction measurements (XRD) and field-emission scanning electron microscopy (FE-SEM) analysis revealed a preferential growth of the nanorod-like structures along the [002] direction. Electrical resistance measurements indicated a good sensitivity to different ozone concentrations (0.06–1.19 ppm) as well as long-term stability over a 6 month period at 250 °C. In addition, it was observed that the nanorods had a good sensitivity to ozone at room temperature when the sensor was exposed to UV illumination. This study provides an easy and efficient way to obtain 1-D ZnO nanorods exhibiting remarkable properties for applications as ozone gas sensing materials.

1. Introduction

Chemical gas sensors have been applied in many areas, such as agriculture, medical diagnosis and detection of environmental pollutants and toxins.[1–4] For gas sensor devices of the highest sensitivity, it is desirable that the sensing material exhibit a large surface-area-to-volume ratio, which favors the adsorption of the gases on its surface.[5] For this reason, sensor devices have been developed based on one-dimensional (1-D) nano-structures, such as nanowires, nanotubes, nanorods and nanobelts.[6–10] Due to their unique characteristics, 1-D ZnO nanostructured material has been widely studied for numerous applications.[8,11] Recently, ZnO nanorods arrays have also received considerable attention in photo-activated applications, in particular, photo-induced superhydrophilicity and photocatalysis.[11]

A number of chemical and/or physical methods have been employed in the production of gas sensor based on 1-D ZnO nanostructure; these include metal–organic chemical vapor deposition (MOCVD),[14] pulsed laser deposition (PLD),[15]

chemical vapor deposition (CVD),[12] molecular beam epitaxy (MBE),[13] sputtering,[16] and electrodeposition.[17]

However, usually these methods require relatively high energy consumption during the synthesis in terms of temperature, pressure and/or vacuum. In contrast, wet chemical methods such as hydrothermal/solvothermal have allowed obtain 1-D ZnO nanostructures using a simple, effective, and reproducible procedure.[18] Although several research groups have studied gas sensors based on 1-D ZnO nanorods *via* hydrothermal treatment,[19,20] few studies have been carried out on the sensing properties of 1-D ZnO nanorods towards ozone gas.

It is important to emphasize that human exposure to ozone gas at the level higher than certain threshold value (0.12 ppm) are likely to result in serious health problems (*e.g.* headache, burning eyes, respiratory irritation and lung damage).[7] In a recent study, Chien and co-workers[12] reported the ozone sensing properties of 1-D ZnO nanorods deposited *via* CVD technique.[12] Their obtained results indicated that 1-D ZnO nanorods exhibited good sensitivity to different ozone concentrations (1 to 2.5 ppm), however, this gas detection range is well above of the minimum recommended level.[12]

We report here on a simple, versatile, and low-cost strategy for obtaining ozone gas sensors based on hierarchical 1-D ZnO nanorod-like structures. To our best knowledge, this is the first study where the hydrothermal treatment method was used to grow 1-D ZnO nanorods directly onto interdigitated electrodes, facilitating the integration of sensing material into the ozone gas sensor device. Electrical resistance measurements at 250 °C showed that the 1-D ZnO nanorods were sensitive even at a lower ozone concentration (0.06 ppm), exhibiting fast response time and long-term stability over a period of 190 days. Additionally, these 1-D ZnO nanorods had relative good ozone

[a]*Instituto de Física de São Carlos, Unversidade de São Paulo, Avenida Trabalhador São-carlense, 400, 13566-590 São Carlos, SP, Brazil*

[b]*LIEC, Instituto de Química, Universidade Estadual Paulista, P.O. Box 355, 14800-900 Araraquara, SP, Brazil. E-mail: lfsilva83@gmail.com*

[c]*EMBRAPA Instrumentação, Rua XV de novembro, 1452, 13560-970 São Carlos, SP, Brazil*

[d]*Aix Marseille Université, CNRS IM2NP (UMR7334), FS St Jérôme S152, Marseille, 13397, France*

gas sensing performance at room temperature when the sample was exposed to UV-light irradiation.

2. Experimental section

2.1. Synthesis procedure

ZnO hexagonal nanorod-like structures were grown *via* the hydrothermal method directly onto a SiO_2/Si substrate with interdigitated Pt electrodes covered with a ZnO seed layer. Initially, a nanocrystalline ZnO thin film, which acted as a seed layer, was deposited onto a pre-cleaned SiO_2/Si substrate with interdigitated Pt electrodes *via* the spin-coating technique.

ZnO hexagonal nanorod-like structures were grown in aqueous solutions using, zinc nitrate $[Zn(NO_3)_2 \cdot 6H_2O$, Aldrich, >99%] and hexamethylenetetramine ($C_6H_{12}N_4$, HMTA, Aldrich, >99%) in a molar concentration of 0.055 mol L^{-1} and 0.1 mol L^{-1}, respectively. The reagents were separately dissolved in deionized water at room temperature and the HMTA solution then slowly added to the zinc solution under continuous stirring. The SiO_2/Si substrate with interdigitated Pt electrodes covered with a ZnO seed layer was placed in a glass bottle containing the resulting transparent solution. The substrate surface containing the ZnO seed layer was face down in the bottom of the glass bottle with a screw cap. Fig. S1† presents in detail the steps taken to obtain the 1-D ZnO nanorod-like structures. The hexagonal 1-D ZnO nanorod growth process was carried out with the glass bottle placed in an electric furnace for 4 hours at 110 °C. The film was removed from the solution when the solution attained room temperature, washed with deionized water and alcohol isopropyl, and dried at 80 °C for 12 hours in an air atmosphere.

2.2. Characterization techniques

One-dimensional ZnO nanostructures were characterized by X-ray diffraction measurements (Diffractometer Rigaku, Ultima IV) with a monochromatic CuKα radiation source. The data were collected in the $2\theta = 20–80°$ range, with a step of 0.02° and a step scanning at 2° min^{-1}. The morphological properties of the 1-D ZnO hexagonal nanorods were analyzed in a field emission scanning electron microscope (FE-SEM, Zeiss Supra35) operating at 10 kV. The average nanorod size was estimated measuring 150 particles from the FE-SEM images. The microanalysis by energy-dispersive X-ray (EDX) spectroscopy was performed in a spectrometer Thermo Scientific (model 6742A).

2.3. Gas sensing measurements

The sample was inserted into a chamber which allowed control of the substrate temperature and ozone concentrations. Ozone gas was formed from oxidizing oxygen molecules of dry air (8.3 cm^3 s^{-1}) by a calibrated pen-ray UV lamp (UVP, model P/N 90-0004-01), providing ozone concentrations from 0.06 to 1.19 ppm. The dry air, containing ozone, was blown directly onto the sample placed on a heated holder. The applied dc voltage was 1 V and the electrical resistance was measured using a Keithley (model 6514) electrometer. The sensitivity (S) was defined as $S = R_{ozone}/R_{air}$, where R_{ozone} and R_{air} are the electric resistance of the sensor exposed to ozone gas and to dry air, respectively.

The sensor response time was defined as the time required for a change in the sample's electrical resistance to reach 90% of the initial value when exposed to ozone gas. In the same way, the recovery time was defined as the time required for the electrical resistance of the sensor to return 90% of the initial value after turning off the ozone gas. To determine the long-term stability over period of 190 days, the sample was stored and exposed to 0.1 ppm of ozone at working temperature of 250 °C every amount of days by measuring the repeated adsorption and desorption cycles (3 cycles were collected).

Gas sensing measurements under UV-light irradiation were performed using a UV-LED (peak wavelength of 351 nm; operating voltage of 3 V) at a working temperature of 26 °C ± 1 °C. The distance between the UV-LED and the sensing material was kept at 10 mm. Initially, the sample was irradiated for 30 min with a UV-LED to stabilize the electrical resistance.

3. Results and discussion

Fig. 1a displays the X-ray diffraction (XRD) pattern of 1-D nanostructure ZnO film. All diffraction peaks were indexed as hexagonal wurtzite structures of ZnO with a $P6_3mc$ space group, according to JCPDS file no. 36-1451. Furthermore, the Zn-K XANES edge spectrum of the 1-D ZnO film revealed that the Zn is tetrahedrally coordinated by four oxygen atoms, exhibiting an oxidation state of 2+,[21] as shown in Fig. S2 (ESI†). The EDX spectrum (Fig. S3†) confirms Zn, and O elements in the ZnO film. The Si and C peaks can be attributed to the silicon substrate and residues of HMTA.

Additionally, the (002) XRD peak presented a higher intensity, showing that the sample was preferentially textured along the *c*-axis, in good agreement with the FE-SEM image (Fig. 1b). FE-SEM images also showed that the ZnO film is composed by uniform hexagonal ZnO nanorod-like structures, as depicted in Fig. 1c and d. The average diameter and length of the nanorods were 160 nm and 2 μm, respectively. The growth process of these ZnO nanorods *via* the hydrothermal method has been investigated in many studies[22-27] and it is well established that it is based on hydrolysis and precipitation reactions.[28]

The electrical resistance of 1-D ZnO nanorods was monitored when exposed to 0.1 ppm of ozone for different periods of time and at a working temperature of 250 °C. As can be seen in Fig. 2, the sample displayed good sensitivity even for shorter exposure times, presented total reversibility and had good stability of the base line. Additionally, the sample did not reach saturation, even for longer exposure times up to 60 seconds, probably due to the high volume/surface ratio of the nanorods.

As is well known, in ozone gas detection, the O_3 gas molecules adsorb on the ZnO surface, implying the formation of an electron-depletion layer due to adsorption of ions, which increases the potential barrier and consequently diminishes ZnO conductivity.[29,30] The gas response of the 1-D ZnO nanorods can be explained by the following reactions,[4]

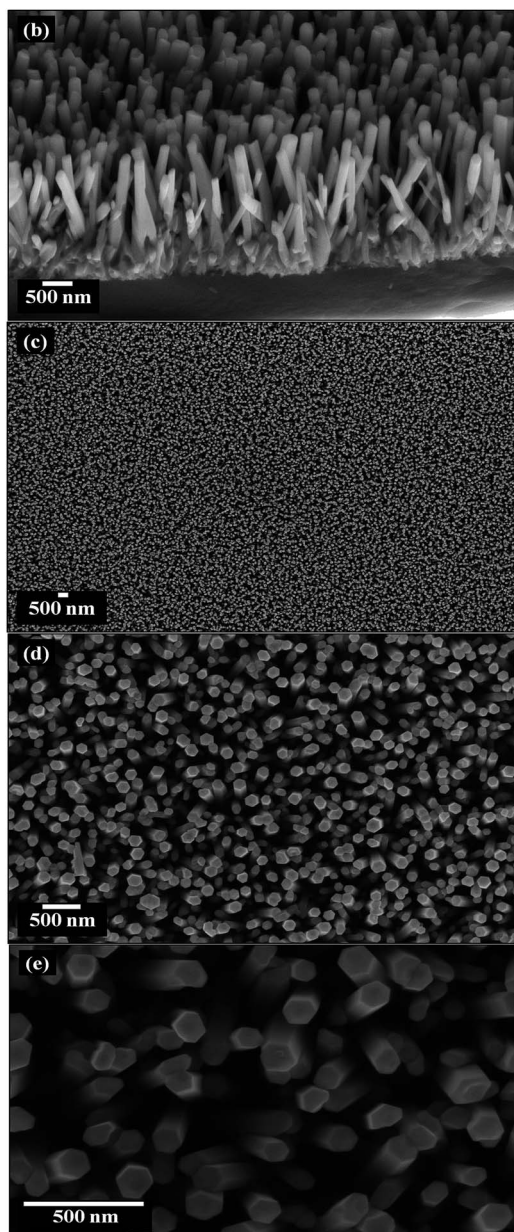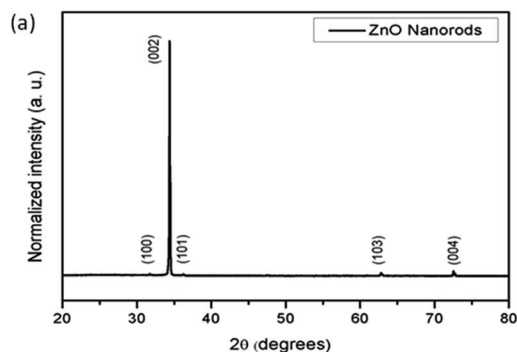$$O_{3(g)} + e^- \rightarrow O_{2(des)} + O_{(ads)}^- \tag{1}$$
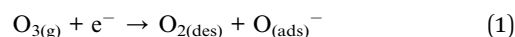
Fig. 1 ZnO nanorods film prepared *via* hydrothermal method. (a) X-ray diffraction pattern, (b) FE-SEM images of cross-section and (c)–(e) surface microstructure.
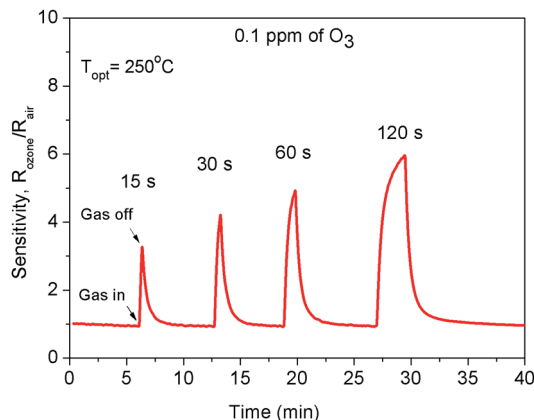

Fig. 2 Ozone gas sensing response of as-prepared ZnO nanorods exposed to 0.1 ppm for different exposure times (15 s, 30 s, 60 s, and 120 s).

In order to determine the optimal working temperature, the sample was exposed for 30 s to 0.1 ppm of ozone at different temperatures. As can be seen in Fig. 3a, the sensitivity of the 1-D ZnO nanorods was highest at 250 °C. This temperature has been seen in the literature.[31] In addition, as displayed in Fig. 3b, the high surface-to-volume ratio of the nanorod-like structures favored the adsorption/desorption processes, presenting a fast
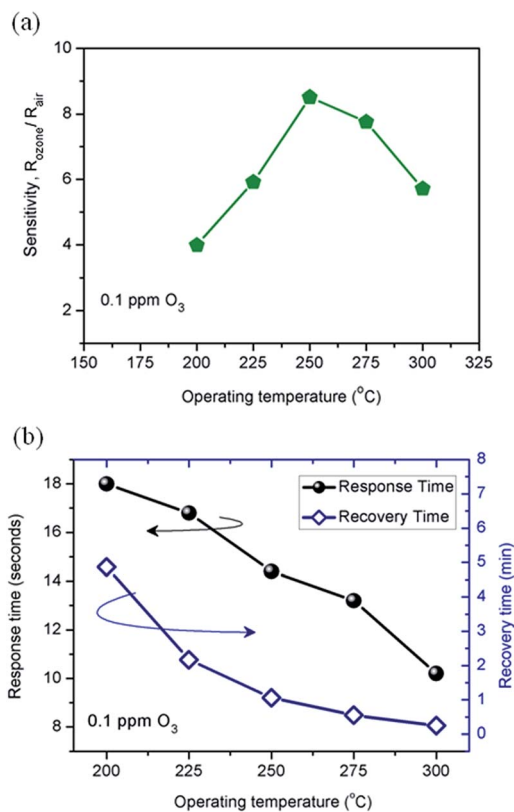

Fig. 3 Ozone gas sensing properties of ZnO nanorods film. (a) Sensitivity and (b) response and recovery time towards 0.1 ppm O_3 at various operating temperatures.

response time (10–18 s) and a recovery time varying from 15 s to 5 min.

The gas sensing response was then studied with different ozone concentrations and at a working temperature of 250 °C, as displayed in Fig. 4. For each measurement cycle, the sample was exposed for 30 s. Fig. 4a shows reversible cycles of the response curve indicating a stable and reproducible response. It can be seen that the resistances of the samples are increased upon to exposure to oxidizing gas, indicating the n-type semiconductor behavior. It is important to note that after several exposure cycles the 1-D ZnO sample detected lower ozone concentration, demonstrating good reversibility. Furthermore, the sensitivity of the 1-D ZnO nanorods increased with ozone concentration and reached saturation at 1.19 ppm, as shown in Fig. 4.

Fig. 5 shows the ZnO nanorods' sensitivity to 0.1 ppm of O_3 at working temperature of 250 °C, over a 190 day period. A slight variation of the gas sensor response, demonstrating long-term stability of the sample, is the average sensitivity value of 5.2 with a standard deviation of 0.5.

Although the results presented here confirm that 1-D ZnO nanorods present a significant sensitivity to ozone around 250 °C, an effort has been made to decrease the operating temperature, and other studies have focused on developing gas sensors that work at room temperature.
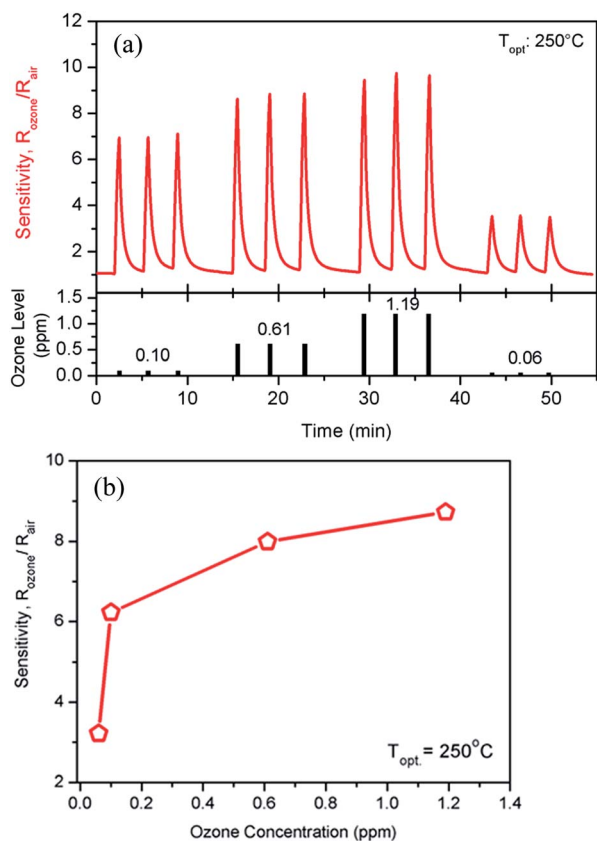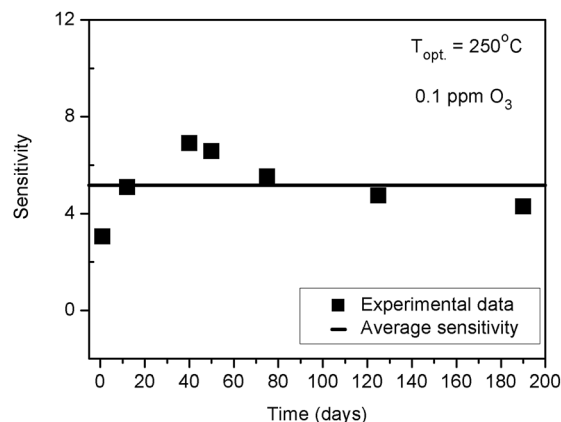

Fig. 5 Stability of the ZnO film during 190 days to 0.1 ppm of ozone.

The sample studied here was initially exposed to ozone at room temperature (around 26 °C) without any illumination, and as can be seen in Fig. 6a, a slight ozone response was observed with a longer recovery time. On the other hand, when the sample was exposed to ozone under UV illumination, Fig. 6b, the sensitivity to ozone gas was enhanced over that without UV light. As showed in Fig. 6b, the 1-D ZnO nanorods exhibited a

Fig. 4 ZnO nanorods at an operating temperature of 250 °C (a) sensitivity and (b) sensitivity *vs.* ozone concentration.
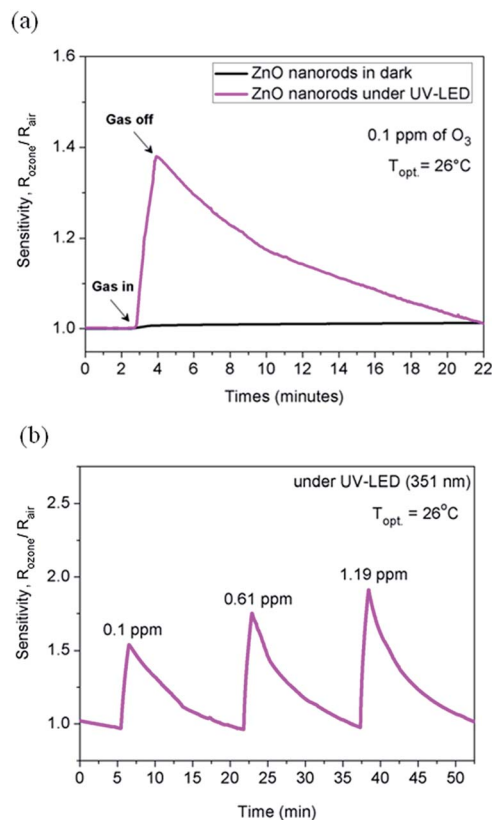

Fig. 6 Ozone sensitivity of ZnO nanorods at room temperature (a) in dark (black curve) and under UV-light exposition (magenta curve) towards 0.1 ppm of O_3 and (b) at various ozone levels operating under UV-light irradiation.

good gas sensing response towards different ozone levels when kept under UV irradiation. The sample exhibited a response time between 40 and 44 s, and a recovery time varying between 9 and 11 min, depending on O_3 level.

The ozone sensing mechanism of ZnO nanorod-like structures under UV light can be explained as follow:

First, when the 1-D ZnO nanorods are exposed to an air atmosphere, oxygen molecules are adsorbed on the different ZnO surfaces,

$$O_{2(gas)} \rightarrow O_{2(ads)}. \quad (2)$$

These oxygen molecules capture free electrons from the ZnO conduction band, forming ionized oxygen anions.[32] At temperatures <150 °C, the ionic species O_2^- are dominant,[30]

$$O_{2(ads)} + e^- \rightarrow O_{2(ads)}^-. \quad (3)$$
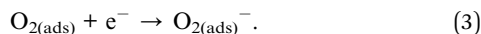
These O_2^- species contribute to form a high-resistance depletion layer in the nanorod surfaces, increasing electrical resistance in the nanorods (Fig. S4†). When the nanorods are exposed to UV irradiation (3.53 eV), electron–hole pairs are photogenerated ($hv \rightarrow h^+ + e^-$) in the ZnO surface, because the photon energy is larger than the ZnO band gap.[31,33,34] The photogenerated holes (h^+) migrate to the ZnO surface, and O_2^- species are photodesorbed,

$$h^+ (hv) + O_{2(ads)}^- \rightarrow O_{2(g)} (hv). \quad (4)$$
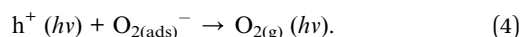
As consequence, the depletion layer is diminished and the remaining unpaired electrons contribute to an increase in the electrical conductivity, as shown in Fig. S4.† Upon exposure to O_3 gas, O_3 molecules adsorb on the ZnO surfaces, as shown in the following reaction:

$$O_{3(g)} + e^- (hv) \rightarrow O_{2(des)} (hv) + O_{2(ads)}^- (hv). \quad (5)$$
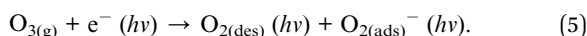
This reaction widens the depletion-layer in the ZnO surface, hindering the flux of charge carriers, and consequently, the electrical resistance is increased when the sensing material is exposed to O_3 gas, as shown in Fig. 6.

4. Conclusions

This work reported a low-temperature way to prepare an ozone gas sensor based on hexagonal 1-D ZnO nanorod-like structures grown *via* a hydrothermal process. Gas sensing measurements showed the great potential of these ZnO nanorods, which display a fast response (of *ca.* 14 s), short recovery time (of *ca.* 60 s), and long-term stability for a period of over 6 months at optimal temperature of 250 °C. In addition to excellent ozone detection at 250 °C, the sample also showed a good sensitivity to ozone at room temperature under UV-light irradiation. This versatile methodology may provide an alternative way to manufacture gas sensor devices, growing them at low temperatures on flexible substrates which operate at room temperature.

Notes and references

1 T. Xiao, X. Y. Wang, Z. H. Zhao, L. Li, L. Zhang, H. C. Yao, J. S. Wang and Z. J. Li, *Sens. Actuators, B*, 2014, **199**, 210–219.
2 Y. L. Tang, Z. J. Li, J. Y. Ma, Y. J. Guo, Y. Q. Fu and X. T. Zu, *Sens. Actuators, B*, 2014, **201**, 114–121.
3 L. Gu, K. Zheng, Y. Zhou, J. Li, X. Mo, G. R. Patzke and G. Chen, *Sens. Actuators, B*, 2011, **159**, 1–7.
4 G. Korotcenkov and B. K. Cho, *Sens. Actuators, B*, 2012, **161**, 28–44.
5 G. J. Cadena, J. Riu and F. X. Rius, *Analyst*, 2007, **132**, 1083–1099.
6 S. Yi, S. Tian, D. Zeng, K. Xu, S. Zhang and C. Xie, *Sens. Actuators, B*, 2013, **185**, 345–353.
7 L. F. da Silva, A. C. Catto, W. Avansi Jr, L. S. Cavalcante, J. Andrés, K. Aguir, V. R. Mastelaro and E. Longo, *Nanoscale*, 2014, **6**, 4058–4062.
8 R. S. Devan, R. A. Patil, J. H. Lin and Y. R. Ma, *Adv. Funct. Mater.*, 2012, **22**, 3326–3370.
9 J. Huang and Q. Wan, *Sensors*, 2009, **9**, 9903–9924.
10 S. Barth, F. H. Ramirez, J. D. Holmes and A. R. Rodriguez, *Prog. Mater. Sci.*, 2010, **55**, 563–627.
11 D. Bekermann, A. Gasparotto, D. Barreca, A. Devi, R. A. Fischer, M. Kete, U. Štangar, O. I. Lebedev, C. Maccato, E. Tondello and G. V. Tendeloo, *ChemPhysChem*, 2010, **11**, 2337–2340.
12 F. S. S. Chien, C. R. Wang, Y. L. Chan, H. L. Lin, M. H. Chen and R. J. Wu, *Sens. Actuators, B*, 2010, **144**, 120–125.
13 B. S. Kang, Y. W. Heo, L. C. Tien, D. P. Norton, F. Ren, B. P. Gila and S. J. Pearton, *Appl. Phys. A*, 2005, **80**, 1029–1032.
14 S. Pati, P. Banerji and S. B. Majumder, *Sens. Actuators, A*, 2014, **213**, 52–58.
15 N. H. Como, S. Moreno, I. Mejia and M. A. Q. Lopez, *Semicond. Sci. Technol.*, 2014, **29**, 085008.
16 C. Y. Lu, S. P. Chang, S. J. Chang, T. J. Hsueh, C. L. Hsu and Y. Z. Chiou, *IEEE Sens. J.*, 2009, **9**, 485–489.
17 S. L. Bai, C. Sun, T. Guo, R. Luo, Y. Lin, A. Chen, L. Sun and J. Zhang, *Electrochim. Acta*, 2013, **90**, 530–534.
18 G. Kenanakis, D. Vernardou, E. Koudoumas, G. Kiriakidis and N. Katsarakis, *Sens. Actuators, B*, 2007, **124**, 187–191.
19 N. Kilinc, O. Cakmak, A. Kosemen, E. Emek, S. Ozturk, Y. Yerli, Z. Z. Ozturk and H. Urey, *Sens. Actuators, B*, 2014, **202**, 357–364.
20 M. R. Alenezi, S. J. Henley, N. G. Emerson and S. R. P. Silva, *Nanoscale*, 2014, **6**, 235–247.
21 H. Liu, F. Zeng, S. Gao, G. Wang, C. Song and F. Pan, *Phys. Chem. Chem. Phys.*, 2013, **15**, 13153–13161.

22 T. L. Sounart, J. Liu, J. A. Voigt, J. W. P. Hsu, E. D. Spoerke, Z. Tian and Y. B. Jiang, *Adv. Funct. Mater.*, 2006, **16**, 335–344.

23 J. Song and S. Lim, *J. Phys. Chem. C*, 2007, **111**, 596–600.

24 K. Govender, D. S. Boyle, P. B. Kenway and P. O'Brien, *J. Mater. Chem.*, 2004, **14**, 2575–2591.

25 R. Savu, R. Parra, E. Joanni, B. Jancar, S. A. Elizário, R. de Camargo, P. R. Bueno, J. A. Varela, E. Longo and M. A. Zaguete, *J. Cryst. Growth*, 2009, **311**, 4102–4108.

26 S. V. Costa, A. G. Gonçalves, M. A. Zaguete, T. Mazon and A. F. Nogueira, *Chem. Commun.*, 2013, **49**, 8096–8098.

27 Y. V. Kaneti, Z. Zhang, J. Yue, Q. M. D. Zakaria, C. Chen, X. Jiang and A. Yu, *Phys. Chem. Chem. Phys.*, 2014, **16**, 11471–11480.

28 X. D. Yan, Z. Li, R. Chen and W. Gao, *Cryst. Growth Des.*, 2008, **8**, 2406–2410.

29 D. Barreca, D. Bekermann, E. Comini, A. Devi, R. A. Fischer, A. Gasparotto, C. Maccato, C. Sada, G. Sberveglieri and E. Tondello, *CrystEngComm*, 2010, **12**, 3419–3421.

30 H. J. Kim and J. H. Lee, *Sens. Actuators, B*, 2014, **192**, 607–627.

31 M. Bendahan, J. Guerin, R. Boulmani and K. Aguir, *Sens. Actuators, B*, 2007, **124**, 24–29.

32 J. Gong, Y. Li, X. Chai, Z. Hu and Y. Deng, *J. Phys. Chem. C*, 2010, **114**, 1293–1298.

33 S. Park, S. An, Y. Mun and C. Lee, *ACS Appl. Mater. Interfaces*, 2013, **5**, 4285–4292.

34 Y. Mun, S. Park, S. An, C. Lee and H. W. Kim, *Ceram. Interfaces*, 2013, **39**, 8615–8622.